CHEMICAL ENGINEERING TRANSACTIONS
VOL. 62, 2017
A publication of AIDIC
The Italian Association of Chemical Engineering
Online at www.aidic.it/cet
Guest Editors: Fei Song, Haibo Wang, Fang He

ISBN 978-88-95608- 60-0; **ISSN** 2283-9216
DOI: 10.3303/CET1762012

The Properties of Heightened Temperature Curing Steel Slag – Ground Blast Furnace Slag Cementitious Material without Clinker

Dongxia Yuan[a], Xiaoying Liang[a*], Xiaoran Lin[a], Changlong Wang[a,b,c], Shenhua Jiao[d]

[a]School of Civil Engineering, Hebei University of Engineering, Handan 056038, China
[b]Jiangxi Key Laboratory of Mining Engineering, Jiangxi University of Science and Technology, Ganzhou 341000, China
[c]Tianjin Sunenergy Sega Environmental Science & Technology Co. Ltd, Tianjin 300000, China
[d]China Ordnance Industry Survey and Geotechinical Institute, Beijing 100053, China
844065183@qq.com

Orthogonal tests were conducted in this paper to study the mechanical properties of the heightened temperature curing steel slag (SS)-ground blast furnace slag (GBFS) cementitious materials without clinker based on four factor: A) the mass ratio of SS/GBFS; B) the mixing milling time of the cementitious materials; C) the mass ratio of $Ca(OH)_2$/gypsum (from flue gas desulfurization waste, FGDW); D) curing temperature. The hydration products and microstructure of the heightened temperature curing SS-GBFS system was also studied. When the four factors are 1:2, 480 m^2 kg^{-1}, 2:1 and 35 ºC, respectively, the highest compressive strength was observed with the values of 18.36 MPa, 26.89 MPa and 45.32 MPa at the ages of 3 days, 7 days and 28 days, respectively. The influence of the four factors on the mechanical properties is in the order of D > A > B > C. The results from X-ray diffraction (XRD) and scanning electron microscope (SEM) indicate that ettringite and C-S-H form from the reactions between C_2S from SS and amorphous phases from GBFS, and FGDW during hydration, which greatly contributes to the early-age strength. As the curing time increases, more ettringite forms due to the reaction of SO_4^{2-} from FGDW, OH^- from $Ca(OH)_2$ and AlO_2^- from GBFS, and the formed ettringite (AFt) intervened with C-S-H gels, which provides the framework of the microstructure and thus improves the strength of the specimens.

1. Introduction

Currently, fly ash (FA) and ground granulated blast furnace slag (GGBFS) are the most widely applied mineral admixtures in the production of cement and concrete. Although the diminution of early strength of concrete owing to the partially substituted cement, these two admixtures can improve the properties of concrete, such as decreasing hydration-induced temperature rise, improving the workability of fresh concrete, reducing the cracking risk, improving durability, and so on (Upadhyaya et al., 2015). In actual concrete industrial production, the combination of FA and GBFS can further improve many properties of concrete, so it is very common to use FA and GBFS in concrete production (Zhao et al., 2015). By the wide application of FA and GBFS in concrete and cement, they have become scarce resources in many Chinese cities, and the price is also rising. At present, it is the consensus that the cement and concrete industry are developing towards the direction of “low carbon”. With the improvement of concrete strength grade, more and more cementitious materials are consumed during the production of concrete. The massive use of mineral admixtures is crucial to the “low carbon” development of cement and concrete. Therefore, it is very meaningful to develop and utilize mineral mixtures that can be applied in massive amount and various environments.
In the slag of steel industry, steel slag (SS) mainly comes from smelting fluxes (e.g. iron ore, dolomite and limestone) added during the steelmaking process, the slagging materials added to adjust the properties of steel, and the impurities separated from the two non-molten liquid phase furnace burdens melted at high temperature. The amount of SS discharged is about 12 %-20 % of crude steel production (Zhang et al., 2012).

Please cite this article as: Dongxia Yuan, Xiaoying Liang, Xiaoran Lin, Changlong Wang, Shenhua Jiao, 2017, The properties of heightened temperature curing steel slag – ground blast furnace slag cementitious material without clinker, Chemical Engineering Transactions, 62, 67-72 DOI:10.3303/CET1762012

In China, 80 million tons of SS are produced each year, and the accumulated amount is about 500 million tons. And the utilization rate is less than 40 % (Li et al., 2011), which is far below the target rate of 75 % in the utilization of massive solid by-products during China's 12th five-year plan. According to the different processes of steel making, SS can be categorized as converter slag, casting slag, electric furnace slag, pre-treatment slag, refining furnace slag, and so on. The amount of converter slag accounts for more than 70 % of the total in China. The utilization of SS mainly includes the applications in producing metallurgical raw materials, subgrade engineering, engineering backfills, innovative building materials, glass-ceramics, and environment and agriculture fields. However, less than 10% of the total amount are being applied to concrete industries (Wang, 2010; Pasetto and Baldo, 2010; Zhang et al., 2012) indicated that SS be used in concrete. The mineral phases of SS include calcium aluminates (C_3A, $C_{12}A_7$), calcium ferrites (C_4AF, C_2F), calcium silicates (C_3S, C_2S), RO phase (CaO-MgO-MnO-FeO solid solution), free MgO, free CaO, Fe_3O_4, and so on (Liu et al., 2014). (Yan et al., 2014).. The chemical composition of SS is mainly CaO, SiO_2, Fe_2O_3, MgO with a small amount of Al_2O_3, MnO_2, P_2O_5 (see Figure 1) (Peng and Huang, 2010). Similar to cement, SS can react with water to form $Ca(OH)_2$, C-S-H gels, C-S-A-H gels, C-A-H, and so on (Wang et al., 2012).. Thus, SS is able to be considered as a supplemental cementitious materials.

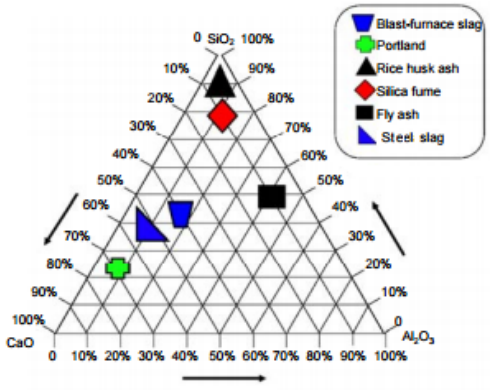

Figure 1: Comparison of compositions of SS, GGBFS and cement (Peng and Huang, 2010).

Recently, Chinese government has implemented a series of policies to motivate the reutilization of SS and GBFS mainly as mineral admixtures of construction materials after grinding. (Wang et al., 2012) mainly used SS, GBFS and 1% cement clinker to prepare the extremely low cement clinker artificial reefs, which has good mechanical properties, low autogenous shrinkage and good compatibility with the marine environment. (Li et al., 2010) used SS, GBFS and cement clinker to prepare a composite mortar with a compressive strength of 50 MPa at 28 days; however, the amount of cement clinker accounts for 80% of the total in the system, which indicates that SS and GBFS were not properly utilized in the above cementitious materials. (Li et al., 1994) used SS and GBFS to prepare the cementitious materials without cement clinker, which has a compressive strength of 46 MPa at 28 days; however, no heightened temperature curing was involved. It is meaningful to study the influence of heightened temperature curing on the property development of the SS-GBFS cementitious materials in some specific aspects. For example, as of engineering filling in mines, the temperature increases as the depth increases, which is beneficial in activating the SS-GBFS cementitious materials without cement clinker based on Arrhenius equation. This paper studies the hydration mechanics and properties of heightened temperature curing SS-GBFS cementitious materials without cement clinker, which will provide the theoretical foundation for its application in practice.

2. Materials and Experimental methods

2.1 Materials

Steel slag (SS). SS used was basic oxygen furnace steel slag without hot closed treatment technology which complies with the Chinese National Standard GB/T 20451-2006, its chemical composition is shown in Table 1. The main chemical composition of SS is CaO (43.73 % w.t.), followed by the residual iron in the steel slag (14.42 % w.t.). SS has higher contents of Fe and Mg and lower contents of Si and Ca. The f-CaO content and f-MgO content in SS are 1.21 % and 0.81 % w.t., respectively. The activity of SS can be partially reflected by the alkalinity calculated from the chemical composition of SS. In China, SS alkalinity is defined by the method of (Mason, 1944). ($CaO/(SiO_2+P_2O_5)$), and divided into three categories: low alkalinity slag (alkalinity <1.8), medium alkalinity slag (alkalinity = 1.8~2.5) and high alkalinity slag (alkalinity> 2.5). In this paper, the alkalinity

of SS is 2.48, which falls in the middle range. The f-CaO content and alkalinity of SS satisfies the requirements in Steel Slag Powder Used for Cement and Concrete (GB/T20491-2006) that f-CaO content should not exceed 3% w.t. and the alkalinity should not fall below 1.8. According to the particle size distribution of SS listed in Table 2, the particles within the size range of 0.30~9.50 mm accounts for 91 % of the total, which indicates that SS needs crushing before grinding. The mineral phases of steel slag are shown in Figure 2(a). The mineral phases of steel slag include C_2S ($2CaO{\cdot}SiO_2$), C_3S ($3CaO{\cdot}SiO_2$), C_2F ($2CaO{\cdot}Fe_2O_3$), $C_{12}A_7$ ($12CaO.7Al_2O_3$), RO phase (CaO-MgO-MnO-FeO solid solution), $Ca_2Al_2Si_3O_{12}$, Fe_3O_4, free Cao (f-CaO) and free MgO (f-MgO), among which C_2S, C_3S and RO phase are the main phases. A small amount of C_4AF ($4CaO{\cdot}Al_2O_3{\cdot}Fe_2O_3$) can be obtained in SS due to the replacement of Al in C_2F. Considering that Al atoms are mainly in the phases of $C_{12}A_7$ and $Ca_2Al_2Si_3O_{12}$, the amount of C_4AF is small.

Table 1: Chemical composition of raw materials (% w.t.)

Materials	SiO_2	Al_2O_3	Fe_2O_3	FeO	MgO	CaO	Na_2O_{eq}	MnO	P_2O_5	SO_3	Loss
SS	14.52	5.64	13.58	6.32	8.66	43.73	0.30	0.74	3.11	1.54	1.38
GBFS	36.97	11.60	0.30	0.33	4.24	41.41	0.69	0.39	0.25	2.03	0.30
FGDW	3.16	1.35	0.47	0.09	7.49	33.38	0.25	-	0.13	45.70	8.28

Note: $Na_2O_{eq}=Na_2O+0.658K_2O$.

Table 2: Particle size distribution of SS and GGBFS (% by mass)

Materials	Particle size /mm									
	+9.50	4.75~9.50	2.36~4.75	1.18~2.36	0.60~1.18	0.30~0.60	0.15~0.30	0.075~0.15	0.0375~0.075	-0.0375
SS	4.11	31.41	23.12	15.46	12.04	8.97	4.89	—	—	—
GGBFS	—	—	10.12	27.61	33.07	21.16	4.24	2.52	1.28	—

Ground blast furnace slag (GBFS). Its chemical composition and particle size distribution are shown in Table 1 and Table 2, respectively. The main chemical composition, SiO_2 and CaO, in GBFS is 36.97 % and 41.41 % w.t., respectively. According to the particle size distribution of GBFS listed in Table 2, the particles within the size range of 0.30~2.36 mm accounts for 81.84 % of the total, which indicates that GBFS needs crushing before grinding. The mineral phases of GBFS are shown in Figure 2(b). Figure 2(b) shows the mineral phase of GBFS is gehlenite ($2CaO{\cdot}Al_2O_3{\cdot}SiO_2$).

Gypsum of flue gas desulfurization waste (FGDW). Its chemical compositions are listed in Table 1, the primary mineral phase of FGDW is $CaSO_4{\cdot}2H_2O$. The specific surface area of the FGDW is 240 $m^2\ kg^{-1}$ and 0.08 mm sieve residual is less than 7.9 %.

Sand. ISO standard sand will be used as fine aggregate in mortar.

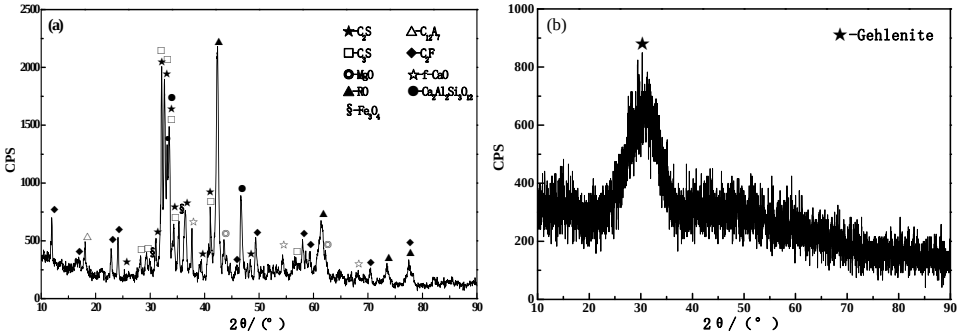

Figure 2: XRD pattern of SS, GBFS and FGDW: (a)-SS, (b)-GBFS.

2.2 Experimental methods

2.2.1 Preparation of SS-GBFS cementitious materials

Firstly, SS, GBFS and FGDW were dried in oven (CS10-3E) at 105 ºC for 24 h to achieve a moisture content less than 1 % w.t. Then they were separately grinded with WL-1 small ball grinder (5 kg, SM Φ500 mm×500 mm) at the speed of 48 r·min-1. GBFS was grinded for 60 mins to achieve a fineness of 450 $m^2\ kg^{-1}$, then

grinded GBFS was mixed together with SS at specific ratios. The mixtures were grinded for 40 mins, 60 mins and 80 mins. FGDW was grinded to a fineness of 380 m^2 kg^{-1}. $Ca(OH)_2$ (AR) was also used.

2.2.2 Preparation of paste and mortars

Pastes: The above mixed well cementitious materials were used to cast pastes according to Chinese Standard GB/T1346-2001. The fresh paste was cast into molds with the dimension of 30 mm×30 mm×50 mm, and then cured in moist room (RH>90%, 20±1 °C) for 1 day. Then the demolded specimens were cured in different curing room until 28 days at the temperatures of 20 °C, 30 °C and 35 °C, respectively.

Mortars: The above mixed well cementitious materials were used to cast pastes according to Chinese Standard GB/T17671-1999. The fresh mortar was cast into molds with the dimension of 40 mm×40 mm×160 mm, and then cured in moist room (RH>90%, 20±1 °C) for 1 day. Then the demolded specimens were cured in different curing room until 28 days at the temperatures of 20 °C, 30 °C and 35 °C, respectively.

2.2.3 Property characterizations

The specific surface area (SSA) of materials were measured using dynamic specific surface area analyzer (SSA-3200). The compressive strength and flexural strength of the mortars were tested according to Chinese Standard GB/T 17671-1999. The strength was measured using hydraulic pressure testing machine (YES-300) with a maximum load of 300 KN and a loading rate of 2.0±0.5 kN/s. The XRD spectra were obtained using a D/Max-RC diffractometer (Japan) with Cu-Kα radiation, voltage of 40 kV, current of 150 mA and *2θ* scanning ranging between 10 °~70 °or 10 ° ~ 90 °. And the wavelength is 1.5406 nm. SEM observation was performed to analyze the hydration products of the paste samples using a Zeiss SUPRA^{TM}55 scanning electron microscope (SEM) coupled with a Be4-U92 energy spectrum.

3. Results and discussion

3.1 Orthogonal tests

Based on the mixture proportions and the previous testing experience, orthogonal test for the compressive strength in this paper was designed as 4 factor by 3 levels as listed in Table 3: A) the mass ratio of SS/GBFS; B) the mixing milling time of the cementitious materials; C) the mass ratio of $Ca(OH)_2$/gypsum (FGDW); D) curing temperature. The experimental results were analyzed by the commonly used efficiency coefficient method.

Table 3: Four factors with three levels in the orthogonal test

Level	Factor			
	A	B	C	D
1	1:2	40	4:1	20
2	8:13	60	2:1	30
3	2:3	80	8:7	35

Table 4: The strength, efficacy coefficient and overall efficacy coefficient of the mortars in the orthogonal tests

NO.	1	2	3	4	Compressive strength /MPa			Efficacy coefficient			Overall Efficacy coefficient
	A	B	C	D	3 d	7 d	28 d	d1	d2	d3	$d = \sqrt[3]{d_1 d_2 d_3}$
1	1(1:2)	1(40)	1(4:1)	1(20)	7.58	20.99	33.55	0.44	0.82	0.79	0.66
2	1(1:2)	2(60)	2(2:1)	2(30)	14.02	21.19	36.91	0.82	0.83	0.87	0.84
3	1(1:2)	3(80)	3(8:7)	3(35)	17.10	24.92	40.26	1	0.97	0.95	0.97
4	2(8:13)	1(40)	2(2:1)	3(35)	16.13	25.57	42.34	0.94	1	1	0.98
5	2(8:13)	2(60)	3(8:7)	1(20)	6.15	11.90	19.68	0.36	0.47	0.46	0.43
6	2(8:13)	3(80)	1(4:1)	2(30)	11.38	23.40	29.15	0.67	0.92	0.69	0.75
7	3(2:3)	1(40)	3(8:7)	2(30)	8.40	18.81	26.87	0.49	0.74	0.63	0.61
8	3(2:3)	2(60)	1(4:1)	3(35)	10.14	20.67	29.53	0.59	0.81	0.7	0.69
9	3(2:3)	3(80)	2(2:1)	1(20)	5.08	15.59	22.27	0.3	0.61	0.53	0.46
K1	2.47	2.25	2.10	1.55							
K2	2.16	1.96	2.28	2.20				K1+K2+K3=6.39			
K3	1.76	2.18	2.01	2.64							
R	0.71	0.29	0.27	1.09							

Table 4 lists the measured strength and the efficiency coefficient of the orthogonal tests. It indicates that the mortar in NO. 4 (A2B1C2D3) test has the highest compressive strength at 28 days. Based on the analysis of variance R, the importance of the four factors is in the order of D > A > B > C. According to K value, the best testing condition is A1B1C2D3. Due to the dramatic influence of the factor A (the mass ratio of SS/GBFS), the testing condition is optimized to be A1B1C2D3 (NO. 10 test), in which the compressive of mortar is 18.36 MPa, 26.89 MPa and 45.32 MPa at the ages of 3 days, 7 days and 28 days. And the hydration products will be analyzed for the corresponding paste of NO. 10 mortar.

3.2 XRD analysis of hydration products

Figure 3 shows the XRD patterns of NO. 10 paste at the ages of 3 days, 7 days and 28 days. The early age strength comes from the formation of ettringite (AFt, $3CaO{\cdot}Al_2O_3{\cdot}3CaSO_4{\cdot}32H_2O$) phase. C_2S in SS and amorphous phases can react with gypsum to form AFt and C-S-H gel (the broad projection at 20~50 ° 2θ in Figure 3), which contributes to the strength of the system. As the hydration proceeds, the peak intensity of gypsum (33.4° and 43.9 ° 2θ) dramatically decreases, as well as those of $Ca(OH)_2$ due to the reactions of sulfate and alkali activation during hydration. More AFt forms due to the reaction of SO_4^{2-} from FGDW, OH^- from $Ca(OH)_2$ and AlO^{2-} from GBFS, and the formed AFt intervened with C-S-H gels, which provides the framework of the microstructure and thus improves the strength of the specimens in the long term.

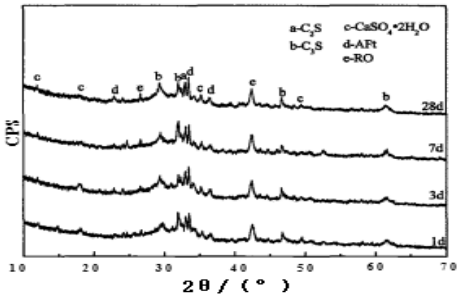

Figure 3: XRD spectras of steel cementitious materials hydrated at various ages.

3.3 SEM analysis of the hydration products

Figure 4 and Figure 5 shows the SEM images of NO. 10 paste at the age of 3 days and 28 days, respectively. As shown in Figure 4(b), C-S-H formed at the age of 3 days, surrounded by a small amount of AFt. Mark “A” in Figure 4(a) is unreacted gypsum surrounded by AFt. Figure 5(a) indicates the proper intervention of C-S-H gels and AFt phases. Compared to Figure 4, more needle-shaped AFt formed (about 5 μm), which is the source of the long-term strength.

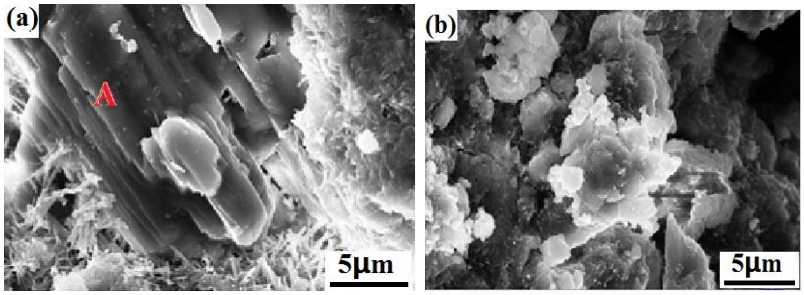

Figure 4: SEM images of hydrated pastes at the age of 3 days.

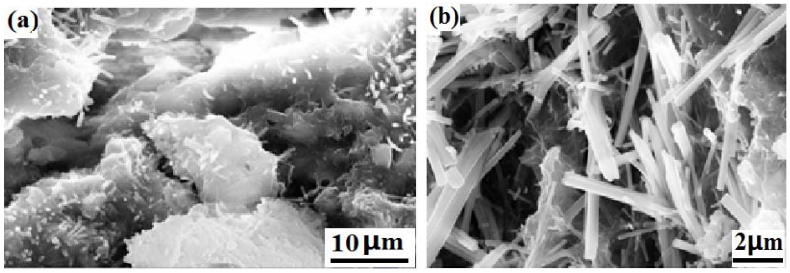

Figure 5: SEM images of hydrated pastes at the age of 28 days.

4. Conclusions

(1) The heightened temperature curing SS-GBFS mortar without clinker based achieved the highest strength of 18.36 MPa, 26.89 MPa and 45.32 MPa at the ages of 3 days, 7 days and 28 days, respectively, as the mass ratio of SS/GBFS (A), the mixing milling time (B), the mass ratio of $Ca(OH)_2$/gypsum (C), and curing temperature (D) are 1:2, 480 m^2 kg^{-1}, 2:1 and 35 ºC, respectively. The influence of the four factors on the mechanical properties is in the order of D > A > B > C.

(2) The results from X-ray diffraction (XRD) and scanning electron microscope (SEM) indicate that AFt and C-S-H gels form from the reactions between C_2S from SS and amorphous phases from GBFS, and FGDW during hydration, which greatly contributes to the early-age strength. As the curing time increases, more AFt forms due to the reaction of SO_4^{2-} from FGDW, OH^- from $Ca(OH)_2$ and AlO^{2-} from GBFS, and the formed AFt intervened with C-S-H gels, which provides the framework of the microstructure and thus improves the strength of the specimens.

(3) The heightened temperature curing dramatically increase the early age compressive strength of SS-GBFS cementitious materials, which provides the new ideology for the reutilization of SS and GBFS in some areas.

Acknowledgments

The authors gratefully acknowledge financial support from China Postdoctoral Science Foundation (2016M602082), supported by Science and Technology Research Project of Higher Education Universities in Hebei Province (ZD2016014, QN2016115), supported by Construction Science and Technology Foundation of Hebei Province (2012-136), supported by Handan Science and Technology Research and Development Plan Program (1621211040-3), supported by Jiangxi Postdoctoral Daily Fund Project (2016RC30).

Reference

Li D. X., Wu X. Q., Fu J. H., 1994, Study on steel slag and slag cement without clinker, Cement and Lime, (6), 10-13.

Li H., Qiu Y., Song Q., 2010, Research on the effect of the pore structure on the strength of the slag and steel slag cement, Concrete, 45-47.

Li J. X, Wei J. X., Zhang T.S., 2011, Structural characteristics and hydration kineties of modified steel slag, Cement and Concrete Research, 41(3), 324-329, DOI: 10.1016/j.cemconres.2010.11.018.

Liu S.J., Hu Q.Q., Zhao F.Q., Chu X.M., 2014, Utilization of steel slag, iron tailings and fly ash as aggregates to prepare a polymer-modified waterproof mortar with a core–shell styrene–acrylic copolymer as the modifier, Construction and Building Materials, 72, 15-22, DOI: 10.1016/j.conbuildmat.2014.09.016.

Mason, B., 1944, The constitution of some open-heart slag, Journal of Iron and Steel Institute, 11, 69-80.

Pasetto M., Baldo N., 2010, Experimental evaluation of high performance base course and road base asphalt concrete with electric arc furnace steel slag, Journal of Hazardous Materials, 181(1-3), 938-948, DOI: 10.1016/j.jhazmat.2010.05.104.

Peng Y.C., Huang C.L., 2010, Carbon steel slag as cementitious material for self-consolidating concrete, Journal of Zhejiang University-SCIENCE A (Applied Physics & Engineering), 11(7), 488-494, DOI: 10.1631/jzus.A0900635.

Upadhyaya S., Goulias D., Obla K., 2015, Maturity-based field strength predictions of sustainable concrete using high-volume fly ash as supplementary cementitious material, Journal of Materials in Civil Engineering, 27(5), 69-75, DOI: 10.1061/(ASCE)MT.1943-5533.0001123.

Wang G., 2010, Determination of the expansion force of coarse steel slag aggregate, Construction and Building Materials, 24(10), 1961-1966, DOI: 10.1016/j.conbuildmat.2010.04.004.

Wang Q., Yang J.W., Yan P.Y., 2012, Influence of initial alkalinity on the hydration of steel slag, Science China Technological Sciences, 55(12), 3378-3387, DOI: 10.1007/s11431-012-4830-9.

Yan P.Y., Mi G.D., Wang Q., 2014, A comparison of early hydration properties of cement–steel slag binder and cement–limestone powder binder, Journal of Thermal Analysis and Calorimetry, 115(1), 193-200, DOI: 10.1007/s10973-013-3360-4.

Zhang T.S., Yu Q.J., Wei J.X., 2012, Investigation on mechanical properties, durability and micro-structural development of steel slag blended cements, Journal of Thermal Analysis and Calorimetry, 110(2), 633-639, DOI: 10.1007/s10973-011-1853-6.

Zhao H., Sun W., Wu X.M., Gao B., 2015, The properties of the self-compacting concrete with fly ash and ground granulated blast furnace slag mineral admixtures, Journal of Cleaner Production, 95, 66-74, DOI: 10.1016/j.jclepro.2015.02.050.